pubs.acs.org/est

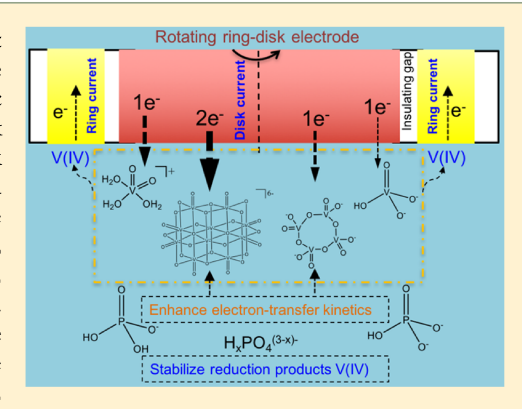
Understanding the Reduction Kinetics of Aqueous Vanadium(V) and Transformation Products Using Rotating Ring-Disk Electrodes

Gongde Chen[†] and Haizhou Liu*,[†]

[†]Department of Chemical and Environmental Engineering, University of California at Riverside, Riverside, California 92521 United

Supporting Information

ABSTRACT: Vanadium(V) is an emerging contaminant in the most recent Environmental Protection Agency's candidate contaminant list (CCL4). The redox chemistry of vanadium controls its occurrence in the aquatic environment, but the impact of vanadium(V) speciation on the redox properties remains largely unknown. This study utilized the rotating ring-disk electrode technique to examine the reduction kinetics of four pH- and concentration-dependent vanadium(V) species in the presence and the absence of phosphate. Results showed that the reduction of VO_2^+ , $H_xV_4O_{12+x}^{(4+x)-}$ (V_4), and HVO_4^{2-} proceeded via a one-electron transfer, while that of $Na_xH_yV_{10}O_{28}^{(6-x-y)-}$ (V_{10}) underwent a two-electron transfer. Koutecky-Levich and Tafel analyses showed that the intrinsic reduction rate constants followed the order of $V_{10} > VO_2^+ > V_4 > HVO_4^{\ 2-}$. Ring-electrode collection efficiency indicated that the reduction product of V_{10} was stable, while those of VO₂⁺, HVO₄²⁻, and V₄ had short half-lives that ranged from



milliseconds to seconds. With molar ratios of phosphate to vanadium(V) varying from 0 to 1, phosphate accelerated the reduction kinetics of V₁₀ and V₄ and enhanced the stability of the reduction products of VO₂⁺, V₄, and HVO₄²⁻. This study suggests that phosphate complexation could enhance the reductive removal of vanadium(V) and inhibit the reoxidation of its reduction product in water treatment.

INTRODUCTION

Vanadium is widely present in the earth crust, with vanadium-(IV) and vanadium(V) being the most common species in the aquatic environment. 1,2 Vanadium(V) is toxic and highly soluble, while vanadium(IV) is less toxic and exists in solid phases at neutral pH. 3,4 The ingestion of vanadium(V) can lead to adverse health effects, including pulmonary tumors.1 Considering the public health risks, the U.S. Environmental Protection Agency included vanadium in the fourth round of its contaminate candidate list (CCL4) and proposed a minimum reporting level of 0.2 μ g/L during the third Unregulated Contaminant Monitoring Rule (UCMR3) program. 5,6 A notification level of 15 μ g/L in drinking water was recommended in California.

Geological weathering of vanadium-containing minerals (e.g., mafic and andesitic rock) naturally releases vanadium into groundwater under oxic and alkaline conditions.⁷ Data collected in California from 1996 to 2007 showed that 18% of public drinking water systems had vanadium levels higher than 21 μ g/L. Up to 220 μ g/L of vanadium has been detected in watersheds containing vanadium-associated ores. The anthropogenic release of vanadium is mainly from the combustion of vanadium-rich fossil fuels, wastewater discharge from the mining, steel, and phosphorus chemical industries.^{2,10} In addition, vanadium-containing minerals, e.g., vanadinite Pb₅(VO₄)₃Cl_(s), was found to cumulate in the corrosion solids

of lead-containing drinking water distribution systems, in which concentrations of vanadium were several orders of magnitude higher than that in the treated drinking water. 11,12 Destabilization of vanadium-containing corrosion solids potentially leaches vanadium and elevates its concentration in treated drinking

Aqueous vanadium(V) exists as monomeric and polymeric oxo-vanadate species depending on pH, vanadium(V) concentration, and ionic strength. 13 Monomeric vanadium(V) species (e.g., H₂VO₄⁻ and HVO₄²⁻) are preferentially present in oxic natural waters. 14 Increasing vanadium concentration promotes their oligomerization into dimers (e.g., H₂V₂O₇²⁻), tetramers (e.g., $V_4O_{12}^{4-}$), and decamers (e.g., $HV_{10}O_{28}^{5-}$). Increasing acidity favors the formation of decamers and VO2+ in water matrix. 15,16 Considering the wide occurrence and regulatory perspective, vanadium removal from drinking water (especially the reductive transformation of vanadium(V) to vanadium(IV) using chemicals, photocatalysts, and microbes with subsequent particle separation) is needed in the future. 2,3,17-23

Prior studies on vanadium(V) chemistry have mostly focused on its application in medical insulin mimetics, flow batteries,

April 19, 2017 Received: September 11, 2017 Revised: Accepted: September 13, 2017 Published: September 13, 2017

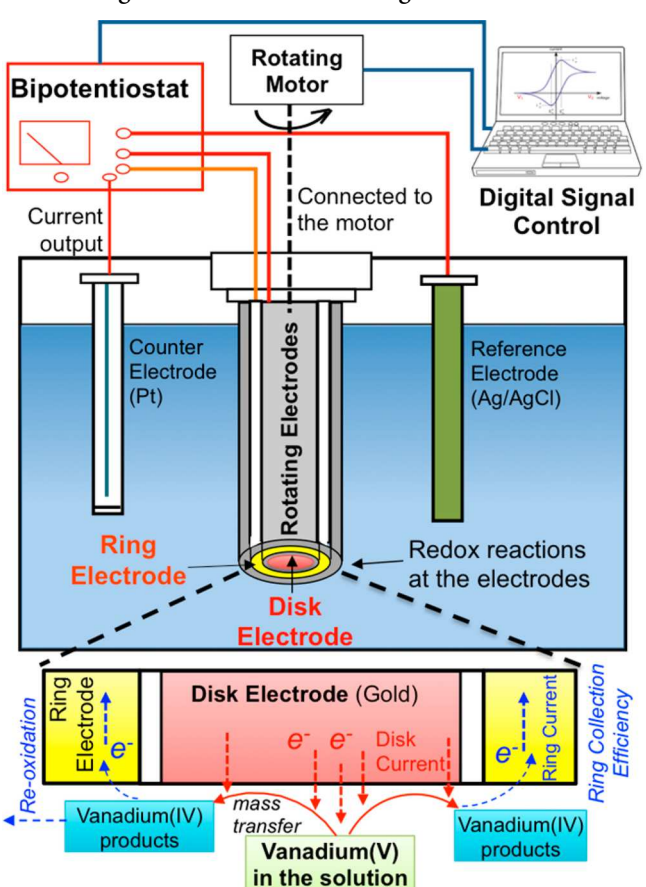
11643

and petroleum refining. 15,16,24,25 Although the redox behaviors of ${\rm VO_2}^+/{\rm VO^{2+}}$ and ${\rm V^{3+}/V^{2+}}$ pairs at extremely acidic conditions have been previously examined for redox flow batteries, the experimental conditions highly deviated from environmentally relevant conditions. 26,27 Vanadium(V) speciation also impacted its reactivity in aquatic environment. 22 Prior study showed that VO₂⁺ cation was reactive toward humic substances, and the reduction of decavanadate by humic substances required its decomposition into VO₂^{+, 22} Decayanadate was also reported to be more prone to reduction than metavanadate (monomer, dimer, tetramer, etc.), and its cage-like structure remained unchanged after its partial reduction.²⁸⁻³¹ However, the structure-redox property relationship, underlying electrontransfer mechanism, and the properties of reduction products remained largely unknown for aquatic vanadium(V) species. In addition, the complexation of organic and inorganic ligands with vanadium(V) affects its redox behavior. 13,32 In particular, vanadium(V) forms stronger complexes with phosphate than other inorganic ligands.³³ Phosphate was ubiquitously present in aquatic system, mainly because of extensive utilization of phosphorus-containing fertilizers with subsequent agriculture runoff.³⁴ In addition, the geological weathering of vanadiumbearing phosphorus mineral ores simultaneously leaches vanadium and phosphate into water matrices. 35,36 Their cooccurrence in aquatic system makes the complexation of vanadium with phosphate environmentally relevant. However, there lacks a fundamental understanding of phosphate impact on reduction kinetics of vanadium(V) species and the stability of their reduction products.

Electrochemical techniques (EC) are robust means to examine the nature of redox-active metal(loid) species and the in situ formation of intermediate products. 37-40 In particular, the rotating ring disk electrode (RRDE) provides insightful information on the electron-transfer kinetics and reaction mechanism. RRDE is an advanced hydrodynamic EC method, in which the substrate is convectively transported to a disk electrode with a potential sweep, and the products generated on the disk is conveyed to the ring with a fixed potential (Scheme 1). However, prior research using RRDE technique to understand the physical and redox properties of environment-relevant species and their transformation products is limited. RRDE technique revealed the generation mechanism of Pb(III) intermediate in the Pb(II)/PbO₂ system and the role of Pb(III) in Pb(II) oxidation in the drinking-water conditions.³⁷ Its application in electrochemical reduction of monoiodoacetic acid and iodoform in the presence of natural organic matter provided insight on their diffusion properties and unveiled their different reduction pathway from Cl- and Brcontaining disinfection by-products.³⁹ For vanadium with multiple valence states and complex speciation, RRDE technique can effectively characterize physical properties and redox behaviors of electrochemically active species, unveil their electron-transfer mechanism, and probe their transformation products.

The objective of this study was to investigate the mechanisms and kinetics of the reduction of pH- and concentrationdependent vanadium(V) species and characterize the formation of intermediate products during the reduction pathway using RRDE techniques combined with conventional cyclic voltammetry (CV). The impact of phosphate on the redox properties of vanadium(V) species was also examined for the aquatic environment with molar ratios of phosphate to vanadium(V) ranging from 0 to 1.

Scheme 1. Principles of Vanadium(V) Reduction on the Disk Electrode and Re-oxidation of Its Reduction Products on the Ring Electrode under Rotating Conditions



MATERIALS AND METHODS

Electrochemical System. EC experiments were carried out in a 150 mL 5-port cell with a gold RRDE working electrode (AFE7R8AUAU), a platinum counter electrode (AFCTR5), and a the Ag/AgCl reference electrode. The disk and ring electrode were controlled by a Pine AFCBP2 bipotentiostat (Pine Research Instrumentation, Durham, NC). The outer diameters of disk and ring electrode was 4.57 and 5.38 mm, respectively, with a gap of 0.18 mm between them. The disk electrode surface area was 0.1642 cm². The theoretical collection efficiency of intermediates by RRDE was determined to be 24% based on the reduction of ferricyanide. The counter electrode was separated from the testing solution using a fritted glass tube. EC potentials were measured and quoted versus the Ag/AgCl reference electrode (+0.197 V versus standard hydrogen electrode, SHE).

Electrochemical Measurements. All solutions were prepared with chemicals (analytical grade) and deionized (DI) water (18.2 M Ω /cm). A 20 mM vanadium(V) solution prepared from NaVO₃ was purged with N₂ gas for 30 min to maintain a negligible level of dissolved O2. A continuous N2 gas flow was positioned above the solution to prevent the ingress of O2 into the solution during EC experiments. pH was fixed at a targeted value of 1, 4, 7, or 11 by adding HClO₄ or NaOH. The predominance diagrams of vanadium(V) (Figures 1 and S1) and vanadium(IV) (Figure S2) were prepared using Visual Minteg software based on the equilibrium reactions and constants (Text S1). In some experiments, 1-20 mM of

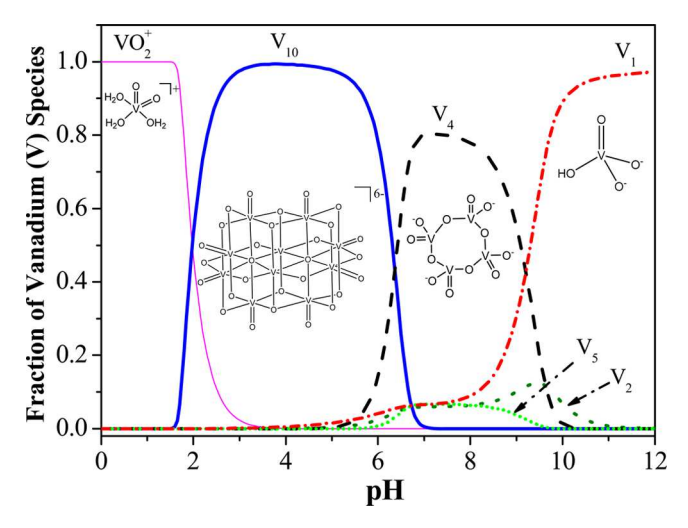


Figure 1. Predominance diagram of vanadium(V) species as a function of pH. Total [vanadium(V)] = 20 mM, [NaClO₄] = 0.6 M, and ionic strength = 0.6 M. V_{10} is a combination of $H_3V_{10}O_{28}^{3-}$, $H_2V_{10}O_{28}^{4-}$, NaHV $_{10}O_{28}^{4-}$, Na $_2V_{10}O_{28}^{4-}$, HV $_{10}O_{28}^{5-}$, and NaV $_{10}O_{28}^{5-}$; V₅ is $V_5O_{15}^{5-}$; V₄ is a combination of $V_4O_{12}^{4-}$ and HV $_4O_{13}^{5-}$; V₂ is a combination of $H_2V_2O_7^{2-}$ and HV $_2O_7^{3-}$; V₁ is a combination of $H_2V_2O_7^{4-}$, HVO $_4^{4-}$, and VO $_4^{3-}$.

phosphate was added. EC experiments were conducted using 0.6 M NaClO₄ as the background electrolyte at 22 \pm 2 $^{\circ}$ C. Changes of pH during EC experiments were negligible. Prior to each experiment, the gold RRDE was polished with alumina slurry and subsequently rinsed with methanol, 0.5 M $\rm H_2SO_4$, and DI water for 30 s each. The reproducibility of the RRDE

surface was confirmed by CV scans with the background electrolyte.

In CV experiments, the disk electrode potential was scanned between -1.35 and 1.30 V, with a scan rate ranging from 25 to 200 mV/s. In RRDE experiments, the electrode rotating speed varied from 400 to 2700 rpm with a constant scan rate of 50 mV/s. When rotating, the potential of disk electrode was scanned within a targeted range, while the ring electrode potential was fixed at a particular value. EC currents on both electrodes were recorded. The collection efficiency of the reduction products was calculated from the ratio of ring electrode current to disk electrode current.

■ RESULTS AND DISCUSSION

Speciation of Concentration- and pH-Dependent Aqueous Vanadium(V). At a fixed ionic strength (0.6 M), the speciation of vanadium(V) is both concentration- and pHdependent. At a low concentration of 2 μ M (102 μ g V/L), only monomeric oxo-vanadate species (VO₂⁺, H₂VO₄²⁻, HVO₄²⁻, and VO₄³⁻) were present (Figure S1A). As concentration increased from 2 to 20 μ M (102 to 1020 μ g V/L), a small portion of $H_2VO_4^-$ dimerized into $H_2V_2O_7^{\ 2-}$ in the pH range from 3 to 9 (Figure S1B). A further increase of the concentration to 0.2 and 2 mM promoted the oligomerization of monomeric species into dimers (V2), tetramers (V4), pentamers (V_5) , and decamers (V_{10}) (Figure S1C,D). Vanadium(V) at near-neutral pHs existed as a mixture of $H_2VO_4^-$, V_2 , V_4 , V_5 , and V_{10} in equilibrium. To create a regime in which only one species predominated at a targeted pH, we further increased vanadium(V) concentration to 20 mM, at which the predominant vanadium(V) species was VO₂⁺, V₁₀,

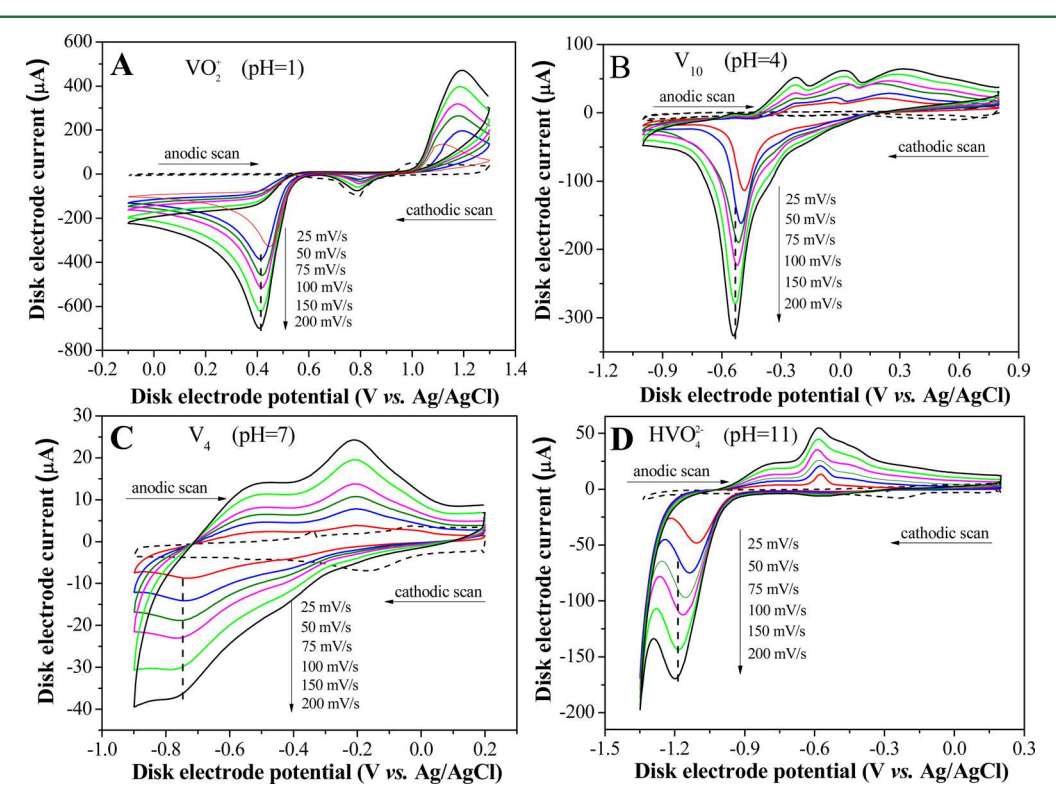


Figure 2. Cyclic voltammetry of vanadium(V) species on a gold disk electrode. Total [vanadium(V)] = 20 mM, [NaClO₄] = 0.6 M, ionic strength = 0.6 M, scan rate = 50 mV/s; dashed lines represent the voltammograms of background electrolyte at 200 mV/s. The cyclic scan on the electrode started in the cathodic direction followed by the anodic direction.

Environmental Science & Technology

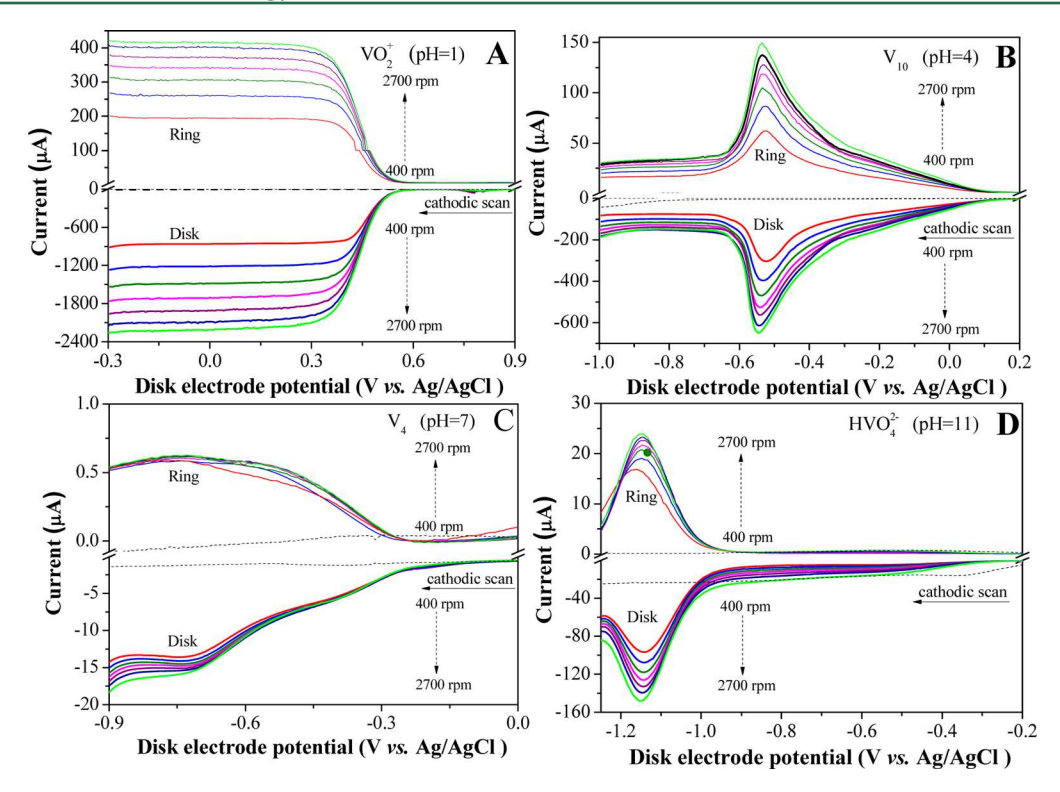


Figure 3. Linear sweep voltammetry of vanadium(V) species on a rotating gold ring-disk electrode. Total [vanadium(V)] = 20 mM, [NaClO₄] = 0.6 M, ionic strength = 0.6 M, and scan rate = 50 mV/s. Ring electrode potential was fixed at 1.3, 1.0, 0.8, and 0.7 V for VO₂⁺, V₁₀, V₄, and HVO₄²⁻, respectively. Dashed lines represent the linear-sweep voltammetry of background electrolyte at 50 mV/s.

 V_4 , and HVO_4^{2-} at pH 1, 4, 7 and 11, respectively (Figure S1E).

As pH and vanadium concentration change, monomeric vanadate V_1 can undergo condensation reactions to form dimers V_2 , tetramer V_4 , pentamers V_5 and decamers V_{10} . 13,15,28,33 With an ionic strength of 0.6 M and total vanadium concentration of 20 mM, the predominant vanadium-(V) species was cationic VO_2^+ at pH less than 2 (Figures 1 and S1E). As the pH raised from 2 to 6, the V_{10} species became predominant. V_{10} had a cage-like molecular structure, with two vanadium atoms located in the center, four in the middle, and the remaining four at the edge. 28 As pH increased from 6 to 9, small oligomers of V_4 species with a cyclic-structure predominated. When the pH was higher than 9, V_1 as HVO_4^{2-} became the major species (Figures 1 and S1E). The presence of V_2 and V_5 species was insignificant. Therefore, the redox behaviors of VO_2^+ , V_{10} , V_4 , and HVO_4^{2-} at pHs of 1, 4, 7, and 11 were subsequently examined using EC tools.

Electrochemical Reduction of Vanadium(V) Species. To examine the redox properties of four vanadium(V) species and their reduction products, the CV at different scan rates was first conducted with a static gold disk electrode. Compared to the background electrolyte, both the cathodic reduction current from vanadium(V) species and the anodic oxidation current from their reduction products increased with the scan rates in vanadium(V)-containing solutions (Figure 2). A well-defined peak was observed at 0.40, -0.53, -0.76, and -1.15 V, corresponding to the EC reduction of VO_2^+ , V_{10} , V_4 , and HVO_4^{2-} , respectively (Figure 2). As the solution pH increased, the onset reduction potential shifted negatively from 0.65 to -0.67 V, suggesting that the thermodynamic feasibility to reduce vanadium(V) followed the order of $VO_2^+ > V_{10} > V_4 > HVO_4^{2-}$. Increasing the scan rates caused negative and positive

shifts of cathodic and anodic peaks, respectively, because faster scan rates shortened the time for electron transfer between vanadium species and the electrode surface. Consequently, a higher over-potential was required to accelerate the reaction kinetics to observe a current response, which caused the shift of both cathodic and anodic peaks. The reduction peak current was linearly correlated with the square root of the scan rate at the static disk electrode (Figure S3). This suggested that electrochemical reduction of vanadium(V) was diffusion-controlled in the static condition.

As the disk electrode started to rotate with a rate from 400 to 2700 rpm, the cathodic current on disk electrode increased (Figure 3). This suggested that mass-transfer limitation was involved in vanadium(V) EC reduction on the disk electrode. Specifically, disk currents corresponding to the reduction of VO₂⁺ started to increase at 0.60 V and plateaued at 0.25 V. With an increase of rotation speed, the disk current in the plateau region increased by 157%, and the ring-electrode current exhibited a similar trend (Figure 3A). For the V_{10} species, disk and ring electrode currents gradually increased from a disk potential of 0.21 V and reached the maximum value at -0.54 V, followed by a drop at a more-negative potential. An increase of rotation speed enhanced the EC current by 113% (Figure 3B). The current drop was likely due to a strong interaction between the V_{10} reduction products and the gold electrode. As the electrode potential became increasingly negative, fast reduction kinetics led to an accumulation of vanadium products on the electrode, and consequently, less electrode surface was available for electron transfer.

The disk electrode current of V_4 reduction increased from a disk potential of -0.21~V and reached a limiting current at -0.74~V (Figure 3C). The reduction current of V_4 increased by 17%, while the ring current remained nearly constant with

varying rotation speed. For HVO_4^{2-} , it exhibited a disk peak centered at -1.15 V, which increased by 54% as the rotation speed increased (Figure 3D). The ultimate reduction product of HVO_4^{2-} was $VO(OH)_3^-$ (Figure S2). At potentials more negative than -1.15 V, a fast reduction of HVO_4^{2-} could accumulate adsorbed $VO(OH)_3^-$ on the electrode surface, which inhibited the further reduction of HVO_4^{2-} and reduced the disk current (Figure 3D). Furthermore, the maximum disk current of V_4 was more than 1 order of magnitude smaller than that of other species (Figure 3C), indicating that V_4 was the least electrochemically active.

Reduction Kinetics and Electron Transfer of Vanadium(V) Species. The kinetics and electron-transfer mechanism of vanadium(V) reduction reactions were investigated based on the CV and RRDE results. The mixed kinetic-diffusion regime for vanadium redox reactions on the rotating disk electrode were analyzed based on the Koutecky–Levich method (eq 1):

$$\frac{1}{i} = \frac{1}{i_{K}} + \frac{1}{i_{D}} = \frac{1}{i_{K}} + \frac{1}{0.62nFA(D)^{2/3}(\omega)^{1/2}(\upsilon)^{-1/6}C_{0}}$$
(1)

where i is the current measured on the disk electrode (A), $i_{\rm K}$ represents the kinetic current in the absence of diffusion limitation (A), $i_{\rm D}$ is the diffusion current (A), n is electrontransfer number of vanadium(V) reduction, F is Faradaic constant (C/mol), A is the electrode surface area (cm²), D is the diffusion coefficient (cm²/s), ω is angular frequency of the rotation (s⁻¹), v is the kinematic viscosity (cm²/s), and C_0 is the bulk concentration (mol/cm³).

Koutecky–Levich plots of RRDE data showed that the reciprocal current (1/i) was linearly correlated with $(\omega)^{-1/2}$, indicating that vanadium(V) reduction was diffusion limited (Figure 4). The slope of the plots was $1/(0.62nFAD^{3/2})$

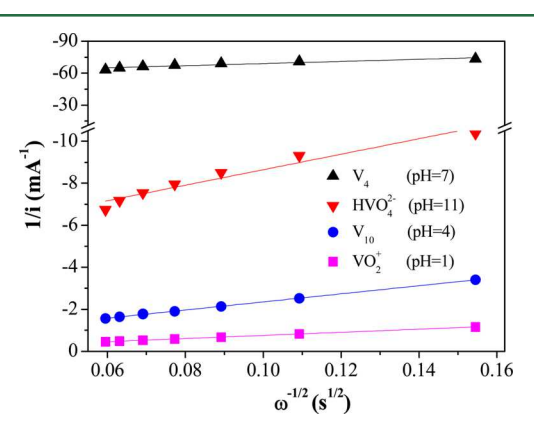


Figure 4. Koutecky–Levich plots of vanadium(V) reduction on a rotating gold ring-disk electrode. Total [vanadium(V)] = 20 mM, [NaClO₄] = 0.6 M, ionic strength = 0.6 M, scan rate = 50 mV/s, and current at different rotation speeds was taken at 0.10, -0.54, -0.74, and -1.15 V for VO₂⁺, V₁₀, V₄, and HVO₄²⁻, respectively.

 $v^{-1/6}C_0$), and the intercept corresponded to the kinetic current in the absence of diffusion limitation. Electron-transfer number of each vanadium(V) species was calculated based on Koutecky–Levich plots and the correlation of reduction peak current versus the square root of scan rates from CV curves (Text S2).

Calculation showed that the first step of EC reduction of VO₂⁺, V₄, and HVO₄²⁻ was approximately a one-electron-

transfer process, while V_{10} reduction was approximately a two-electron-transfer process (Table 1). Prior studies showed that

Table 1. Summary of Electron-Transfer Number, Intrinsic Rate Constants, and Diffusion Coefficients of Vanadium(V) Species and Half-Lives of Their Reduction Products on the Gold Ring-Disk Electrode

pН	vanadium(V) species	electron- transfer number	diffusion coefficient (cm ² /s)	intrinsic rate constant (cm/s)	half-life of reduction products (s)
1	VO_2^+	1.0	5.8×10^{-6}	3.6×10^{-5}	3.5
4	V_{10}	1.5	5.8×10^{-5}	2.6×10^{-3}	213
7	V_4	0.9	1.5×10^{-6}	2.5×10^{-5}	0.08
11	HVO_4^{2-}	1.1	4.7×10^{-7}	3.1×10^{-6}	1.4

 V_{10} was partially reduced by ascorbate and Fe(II) via a two-electron-transfer process and maintained its cage-like original structure. ^{29,30,42} The EC-calculated electron-transfer number of V_{10} reduction was smaller than two (n=1.5) because the reduction current was likely impacted by strong interaction between vanadium reduction products and electrode surface. This was supported by a decrease of reduction current at high over-potentials, i.e., the difference between applied potential and onset reduction potential (Figure 3B).

Based on the calculated electron-transfer number (Table 1) and predicted vanadium(IV) speciation (Figure S2), the EC reduction reactions of four vanadium(V) species are described as follows:

$$VO_2^+ + e^- + 2H^+ \leftrightarrow VO^{2+} + H_2O$$
 (2)

$$HV_{10}^{V}O_{28}^{5-} + 2e^{-} \leftrightarrow HV_{8}^{V}V_{2}^{IV}O_{28}^{7-}$$
 (3)

$$V_4O_{12}^{4-} + e^- + 4H_2O \leftrightarrow VO(OH)_3^- + H_2V_2O_7^{2-} + H_2VO_4^- + OH^-$$
(4)

$$HVO_4^{2-} + e^- + 2H_2O \leftrightarrow VO(OH)_3^- + 2OH^-$$
 (5)

The diffusion coefficient of vanadium(V) species was further calculated using the Levich equation (Text S2), and it followed the order of $V_{10} > VO_2^+ > V_4 > HVO_4^{2-}$ (Table 1). This difference was associated with the limiting ionic equivalent conductivity and ionic charge of vanadium(V) in the solution.⁴³

To gain insight into electron-transfer process involving vanadium(V) reduction at the gold electrode, the intrinsic rate constants (k_0) were calculated based on Bulter–Volmer electrode kinetics. k_0 represents the reduction kinetics of vanadium(V) species in the absence of an over-potential and indicates electron-transfer feasibility between vanadium(V) species and electrode. k_0 is associated with the rate constant at a targeted over-potential (k) and charge-transfer coefficient (α) :⁴¹

$$k_0 = k/\exp\left(-\frac{\alpha F\eta}{RT}\right) \tag{6}$$

 η is the overpotential applied on the electrode, R is the ideal gas constant, and T is the temperature. k was calculated through Koutecky–Levich plots of RRDE data at targeted overpotentials (Text S3 and Figures S4–S5). α was obtained through Tafel analysis of RRDE data at high rotation speeds (Text S3 and Figures S6–S7). α represents the fraction of the total energy change on the electrode that applied to lower the reduction barrier of vanadium(V) species. 41 Calculations

showed that V_{10} had the highest intrinsic rate constant, which was 2 orders of magnitude larger than those of VO_2^+ and V_4 , and 3 orders of magnitude larger than that of HVO_4^{2-} (Table 1).

According to Marcus Theory, the intrinsic rate constant is associated with the interaction of vanadium(V) with electrode surface and the reorganization of vanadium molecules during the reduction reaction. 41 V_{10} had cage-like superstructure with interactive vanadium atoms linked through oxygen atoms, which favored the electron transfer. This structure was not available in VO_2^+ , V_4 and HVO_4^{2-} . In addition, V_{10} underwent much smaller configuration change than the other three species, during the reduction process that also contributed to its largest intrinsic rate constants (eqs 2-5). 28,30,42 Prior study also showed that decavanadate was more active to stimulate NADH oxidation than metavanadate (V₄-dominated) because of fast electron-transfer kinetics in cage-like superstructure. 31 The dioxo ligands in $\mathrm{VO}_2^{\,+}$ and the cyclic structure of V₄ likely made vanadium atoms more intrinsically reducible than that in HVO₄²⁻ Consequently, both species had larger intrinsic rate constants than HVO₄²⁻ (Table

Reoxidation and Stability of Vanadium(IV) Products.

The nature of vanadium(IV) intermediate products from the reduction of VO_2^+ , V_{10} , V_4 , and HVO_4^{2-} was further examined by their collection efficiency on the ring electrode. The vanadium(IV) products was transported via convection from the disk to the ring electrode and reoxidized. The collection efficiency was calculated as the ratio of oxidation current of vanadium(IV) products on the ring electrode to the reduction current of vanadium(V) on the disk electrode (Scheme 1). Results showed that the collection efficiency increased with the ring electrode potential until it reached a plateau, beyond which the oxidation of vanadium(IV) products on the ring electrode was not limited by kinetics (Figure 5). The onset ring electrode

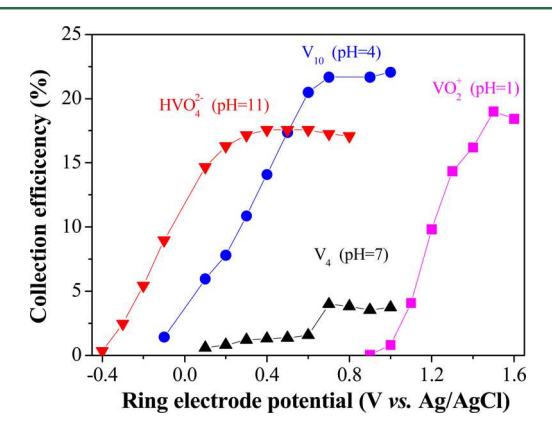


Figure 5. Impact of ring electrode potential on the collection efficient of the intermediate products produced on the gold disk electrode. Total [vanadium(V)] = 20 mM, [NaClO₄] = 0.6 M, ionic strength = 0.6 M, rotation speed = 2400 rpm, and scan rate = 50 mV/s.

potential in response to a discernible collection efficiency represents the thermodynamic oxidation potential of vanadium-(IV) products, i.e., a smaller onset ring electrode potential corresponded to a lower thermodynamic barrier. Based on the correlation of collection efficiency with ring electrode potential, the reduction product of $HVO_4^{\ 2^-}$ was thermodynamically more easily to be reoxidized than that of V_{10} , followed by V_4 and $VO_2^{\ +}$.

Furthermore, the maximal collection efficiency correlated with the stability of vanadium(IV) intermediate products, and their half-lives were subsequently calculated (Text S4). The maximum collection efficiency of vanadium(IV) products of VO_2^+ , V_{10} , V_4 , and HVO_4^{2-} was 22.4%, 23.3%, 4.3%, and 17.1%, respectively (Figure S8). The half-life of their reduction products was 3.5, 213, 0.08, and 1.4 s, respectively (Table 1). Partially reduced V_{10} had a half-life of minutes for reoxidation. V_4 had the most-redox-active and unstable reduction product, which quickly decayed within milliseconds.

Impact of Phosphate on the Reduction of Vanadium-(V) Species. The formation constant between vanadium(V) and phosphate is sufficiently high that the impact of phosphate present in water matrices on the redox properties of vanadium should be considered. To quantify the impact of phosphate on the reduction kinetics of vanadium(V) species, EC reduction rate constants of four vanadium(V) species (k) were calculated from the RRDE data at different phosphate concentrations (Text S3). The results showed that the presence of phosphate accelerated the reduction kinetics of V₁₀ and V₄ but had a minimal impact on that of VO_2^+ and HVO_4^{2-} (rate constant k in Table 2). As molar ratios of phosphate to vanadium(V) increased from 0 to 1, the EC reduction rate constants of V₁₀ and V₄ increased by 53% and 150%, respectively, whereas those of VO₂⁺ and HVO₄²⁻ remained relatively constant (rate constant k in Table 2).

To gain insight into phosphate impact on the rate constants (k) of vanadium(V) species, the intrinsic rate constant (k_0) and charge-transfer coefficient (α) were further calculated. Based on Bulter-Volmer electrode kinetics, k at targeted potentials is associated with k_0 and α (eq 6). Increasing k_0 and α can promote the electron transfer between vanadium(V) and electrode, lower the reduction barrier, and consequently accelerate the reduction kinetics of vanadium(V) species.⁴ Calculation showed that the increase of molar ratios of phosphate to vanadium(V) from 0 to 1 had a negligible impact on k_0 and α of $\mathrm{VO_2}^+$, and thus, its reduction rate constant k was nearly unchanged (Table 2 and Figure S9A). On the contrary, varying molar ratios of phosphate to vanadium(V) from 0 to 1 increased α of V_{10} by 125%, which was consistent with the observed enhancement in V₁0 reduction kinetics at −0.26 V (Table 2 and Figure S9B). Phosphate prominently increased k_0 of V₄ by 4 times, which accounted for the enhanced reduction kinetics of V_4 at -0.30 V (Table 2 and Figure S9C). The presence of phosphate decreased k_0 but increased α of HVO₄²⁻. Consequently, the overall effects of k_0 and α exerted no impact on the reduction rate constants of HVO₄²⁻ (Table 2 and Figure S9D).

The observed phosphate-induced changes on reduction activities of vanadium(V) species were likely associated with vanadium(V)—phosphate complexation. At pH 1, H_3PO_4 (predominant phosphate species; Figure S10) was less likely to form complex with VO_2^+ via ligand exchange, considering its steric hindrance and reluctance to share electrons with vanadium. Therefore, phosphate had a negligible impact on the reduction activity of VO_2^+ (rate constant k in Table 2). At pH 4, VO_2^+ was polymerized to decavanadate V_{10} , and H_3PO_4 deprotonated into $H_2PO_4^-$ (Figure 1 and Figure S10). Prior study reported that phosphate was readily incorporated into polyvanadate ions. 45 $H_2PO_4^-$ likely complexed with the decavanadate V_{10} ions to form anhydrides. 46 The added phosphate group in the structure tended to pull the electrons away from vanadium atoms, lower their electron density and

Table 2. Impact of Molar Ratios of Phosphate to Vanadium(V) ([PO₄]/[V(V)]) on the Kinetic Parameters of Vanadium(V) Species on the Rotating Gold Ring-Disk Electrode^a

	VO ₂ ⁺			V_{10}		V_4		HVO ₄ ²⁻				
[PO ₄]/ [V(V)]	k ₀ (cm/s)	α	k (cm/s)	k ₀ (cm/s)	α	k (cm/s)	k ₀ (cm/s)	α	K (cm/s)	k ₀ (cm/s)	α	K (cm/s)
0	3.6×10^{-5}	0.59	3.9×10^{-3}	2.6×10^{-3}	0.08	1.4×10^{-2}	2.5×10^{-5}	0.23	9.8×10^{-5}	3.1×10^{-6}	0.30	4.8×10^{-4}
0.05	4.1×10^{-5}	0.59	4.3×10^{-3}	2.3×10^{-3}	0.10	1.9×10^{-2}	3.6×10^{-5}	0.21	1.2×10^{-4}	1.2×10^{-6}	0.36	5.1×10^{-4}
0.25	5.2×10^{-5}	0.58	4.8×10^{-3}	6.9×10^{-4}	0.16	1.9×10^{-2}	3.4×10^{-5}	0.18	1.0×10^{-4}	1.1×10^{-6}	0.36	4.8×10^{-4}
0.5	4.2×10^{-5}	0.59	4.4×10^{-3}	5.5×10^{-4}	0.18	2.2×10^{-2}	6.6×10^{-5}	0.19	2.1×10^{-4}	1.0×10^{-6}	0.36	4.3×10^{-4}
1	3.5×10^{-5}	0.60	3.7×10^{-3}	5.6×10^{-4}	0.18	2.2×10^{-2}	9.8×10^{-5}	0.18	2.8×10^{-4}	1.6×10^{-6}	0.33	4.8×10^{-4}

^ak₀: intrinsic rate constants. α: charge-transfer coefficients. k: rate constants of VO₂⁺, V₁₀, V₄, and HVO₄²⁻ at 0.45, -0.26, -0.30, and -1.10 V, respectively. $[PO_4] = 0$, 1, 5, 10, and 20 mM, [V(V)] = 20 mM.

reduction barrier, and consequently facilitate their electron transfer with electrode surface. Increasing molar ratios of phosphate to vanadium from 0 to 1 promoted phosphate complexation with V₁₀. This led to the formation of more reducible vanadium and, thus, increased the reduction kinetics of V_{10} at low over-potentials (rate constant k in Table 2).

As pH further increased to 7, V₄ was the main species (Figure 1) and in fast exchange with mono- and divanadate species at a time scale of milliseconds.⁴⁷ Previous study indicated that H₂PO₄²⁻ and HPO₄⁻ promoted the decomposition of V₄ to H₂VO₄⁻ and induced complexation of H₂VO₄⁻ to form anhydrides (H₂VPO₇²⁻ and HVPO₇³⁻).⁴⁵ Phosphate-induced changes on V₄ made vanadium morereducible and consequently accelerated the reduction kinetics of vanadium(V) as the molar ratios of phosphate to vanadate increased from 0 to 1 (rate constant k in Table 2).⁴⁵ Phosphateenhanced reduction kinetics of V₁₀ and V₄ was consistent with prior observation that phosphate catalyzed the oxidation of NADH by polyvanadate in biological systems.³¹ A further increase of pH to 11 induced the hydrolysis of V₄ to HVO₄²⁻. HVO₄²⁻ rapidly complexed with HPO₄⁻ (the dominant phosphate species; Figure S10) to form unstable anhydride.⁴⁵ The weak interaction of phosphate with HVO₄²⁻ exhibited little impact on the reduction kinetics of HVO_4^{2-} (rate constant k in Table 2).

Furthermore, phosphate affected the stability of vanadium-(V) EC reduction products, i.e., vanadium(IV). As the molar ratio of phosphate to vanadium increased from 0 to 1, ring electrode collection efficiency increased for the reduction products of VO₂⁺, V₄, and HVO₄²⁻ but had minimal change for that of V₁₀ (Figure S11). That indicated that phosphate likely stabilized the reduction products of VO₂⁺, V₄, and HVO₄²⁻ but had little impact on that of V₁₀. The reduction products of VO₂⁺ V₄, and HVO₄²⁻ were VO²⁺, VO(OH)₃⁻, and VO- $(OH)_3^-$, respectively (eqs 2, 4, and 5). For V_{10} , partially reduced product with the original cage-like structure $(HV_8^VV_2^{IV}O_{28}^{7-})$ was generated (eq 3). Prior study demonstrated that VO²⁺ unit could complex with phosphate to form vanadyl-phosphate complexes.⁴⁷ The strong interaction of VO²⁺ with phosphate group in adenosine triphosphate (ATP) inhibited the oxidation of VO²⁺. Phosphate also likely coordinated with VO2+ and VO(OH)3- to form thermodynamically stable complexes. For partially reduced V₁₀ $(HV_8^VV_2^{IV}O_{28}^{7-})$, its intrinsic cage-like structure highly stabilized the reduced vanadium. The data suggested that phosphate had minimal impact on the stability of vanadium(IV) in partially reduced V_{10} (HV₈^VV₂^{IV}O₂₈⁷⁻).

Environmental Implications and Broader Significance.

EC data from this study suggest that the change of vanadium(V) speciation with pH and the presence of phosphate in source water can significantly impact the reactivity of vanadium(V) during the reductive water treatment. Vanadium(V) in acidic wastewater, e.g., wastewater discharged during the extraction of phosphoric acid from vanadiumenriched phosphorus ores and manufacturing of vanadium pentoxide, is expected to have higher reactivity than wastewater in neutral or alkaline conditions. 48 In an aquatic environment with molar ratios of phosphate to vanadium(V) from 0 to 1, e.g., watersheds with remarkably geological weathering of vanadium-bearing minerals, and water bodies contaminated by the point discharge of concentrated vanadium wastewater, phosphate can promote the reduction of vanadium(V), and stabilize vanadium(IV) under oxic environments and, consequently, inhibit the inadvertently reoccurrence of vanadium-(V). Even though the impact of bicarbonate, carbonate, sulfate, and natural organic matters (e.g., humic acid) are not examined in this study, they can potentially affect the reduction kinetics and half-lives of the intermediate products due to complexation reactions. These effects will be examined in future work. Considering the biological effect of vanadium(V) and sensitive response from enzymatic activities, interactions of trace-level vanadium(V) and vanadium(IV) species with environmentrelevant ligands can also be investigated by a simple and fast enzyme kinetic method in future.²

The EC techniques unveiled the redox nature and stability of vanadium species. Current-potential responses on static and rotating electrode combined with classical EC theories allowed the study of diffusivity, electron-transfer kinetics, and product stability of aquatic contaminants. Even though the concentration of vanadium(V) employed in this study is much higher than that in drinking water, the fundamental redox behaviors are the same. Furthermore, the EC techniques developed from this study have broader applications that can be extended to examine other toxic and redox-active contaminants, e.g., chromate, selenate, and halogenated organics. The intrinsic kinetic and thermodynamic nature of electron-transfer processes involving these contaminants obtained from EC tools can guide the design of efficient treatment units to minimize their presence in drinking water.

ASSOCIATED CONTENT

S Supporting Information

The Supporting Information is available free of charge on the ACS Publications website at DOI: 10.1021/acs.est.7b02021.

Additional texts and figures showing the correlation between peak current and scan rates, predominance

diagrams, experimental calculations, half-lives of the intermediate products, experimental material speciation, equilibrium reactions, phosphate and rotation speed impact, and Tafel and Koutecky-Levich plots. (PDF)

AUTHOR INFORMATION

Corresponding Author

*Phone (951)-827-2076; fax: (951)-827-5696; e-mail: haizhou@engr.ucr.edu.

ORCID ®

Haizhou Liu: 0000-0003-4194-2566

The authors declare no competing financial interest.

ACKNOWLEDGMENTS

This study was supported by U.S. National Science Foundation CAREER Program (CBET-1653931) and Early Concept Grants for Exploratory Research Program (CBET-1619915). We thank Dr. Juchen Guo at UC Riverside for suggestions on the data analysis.

REFERENCES

- (1) Howd, R. Proposed notification level for vanadium; California Office of Environmental Health Hazard Assessment: Sacramento, CA
- (2) Sturini, M.; Rivagli, E.; Maraschi, F.; Speltini, A.; Profumo, A.; Albini, A. Photocatalytic reduction of vanadium (V) in TiO2 suspension: Chemometric optimization and application to wastewaters. J. Hazard. Mater. 2013, 254, 179-184.
- (3) Zhang, J.; Dong, H.; Zhao, L.; McCarrick, R.; Agrawal, A. Microbial reduction and precipitation of vanadium by mesophilic and thermophilic methanogens. Chem. Geol. 2014, 370, 29-39.
- (4) Crans, D. C.; Amin, S. S.; Keramidas, A. D. Chemistry of Relevance to Vanadium in the Environment; Advances in Environmental Science and Technology: New York, 1998; vol 30, pp 73-96.
- (5) United States Environmental Protection Agency. Contaminants - CCL 4 . https://www.epa.gov/ccl/chemicalcontaminants-ccl-4 (accessed on 04/10/2017).
- (6) United States Environmental Protection Agency. The Third Unregulated Contaminant Monitoring Rule (UCMR 3) Fact Sheet for Assessment Monitoring (List 1 Contaminants). https://www.epa. gov/sites/production/files/2016-05/documents/ucmr3-factsheet-list1. pdf (accessed on 04/10/2017).
- (7) Wright, M. T.; Belitz, K. Factors controlling the regional distribution of vanadium in groundwater. Groundwater 2010, 48 (4),
- (8) United States Environmental Protection Agency. Presented at the June 16th Public Meeting on Preliminary Regulatory Determinations for the CCL3 . https://www.epa.gov/ccl/slidespresented-june-16th-public-meeting-preliminary-regulatorydeterminations-ccl3.
- (9) Byerrum, R.; Eckardt, R.; Hopkins, L.; Libsch, J.; Rostoker, W.; Zenz, C.; Gordon, W.; Mountain, J.; Hicks, S.; Boaz, T. Vanadium; National Academy of Sciences: Washington, DC, 1974, 584.
- (10) Al-Ghouti, M. A.; Al-Degs, Y. S.; Ghrair, A.; Khoury, H.; Ziedan, M. Extraction and separation of vanadium and nickel from fly ash produced in heavy fuel power plants. Chem. Eng. J. 2011, 173 (1), 191-197.
- (11) Gerke, T. L.; Scheckel, K. G.; Schock, M. R. Identification and distribution of vanadinite (Pb₅(V⁵⁺O₄)₃Cl) in lead pipe corrosion byproducts. Environ. Sci. Technol. 2009, 43 (12), 4412-4418.
- (12) Peng, C.-Y.; Korshin, G. V. Speciation of trace inorganic contaminants in corrosion scales and deposits formed in drinking water distribution systems. Water Res. 2011, 45 (17), 5553-5563.

- (13) Tracey, A.; Crans, D. Vanadium compounds, ACS Symp. Ser., 1998; American Chemical Society: Washington, DC, 1998; pp 308-
- (14) Aureli, F.; Ciardullo, S.; Pagano, M.; Raggi, A.; Cubadda, F. Speciation of vanadium (IV) and (V) in mineral water by anion exchange liquid chromatography-inductively coupled plasma mass spectrometry after EDTA complexation. J. Anal. At. Spectrom. 2008, 23 (7), 1009–1016.
- (15) Crans, D. C.; Smee, J. J.; Gaidamauskas, E.; Yang, L. The chemistry and biochemistry of vanadium and the biological activities exerted by vanadium compounds. Chem. Rev. 2004, 104 (2), 849-902.
- (16) Aureliano, M. Decavanadate: a journey in a search of a role. Dalton Transactions 2009, 42, 9093-9100.
- (17) Guzman, J.; Saucedo, I.; Navarro, R.; Revilla, J.; Guibal, E. Vanadium interactions with chitosan: influence of polymer protonation and metal speciation. Langmuir 2002, 18 (5), 1567-1573.
- (18) Naeem, A.; Westerhoff, P.; Mustafa, S. Vanadium removal by metal (hydr) oxide adsorbents. Water Res. 2007, 41 (7), 1596-1602.
- (19) Peacock, C. L.; Sherman, D. M. Vanadium (V) adsorption onto goethite (α-FeOOH) at pH 1.5 to 12: a surface complexation model based on ab initio molecular geometries and EXAFS spectroscopy. Geochim. Cosmochim. Acta 2004, 68 (8), 1723-1733.
- (20) White, A. F.; Peterson, M. L. Reduction of aqueous transition metal species on the surfaces of Fe (II)-containing oxides. Geochim. Cosmochim. Acta 1996, 60 (20), 3799-3814.
- (21) Wilson, S. A.; Weber, J. H. An EPR study of the reduction of vanadium (V) to vanadium (IV) by fulvic acid. Chem. Geol. 1979, 26 (3), 345-354.
- (22) Lu, X.; Johnson, W. D.; Hook, J. Reaction of vanadate with aquatic humic substances: an ESR and 51V NMR study. Environ. Sci. Technol. 1998, 32 (15), 2257-2263.
- (23) Ortiz-Bernad, I.; Anderson, R. T.; Vrionis, H. A.; Lovley, D. R. Vanadium respiration by Geobacter metallireducens: novel strategy for in situ removal of vanadium from groundwater. Appl. Environ. Microbiol. 2004, 70 (5), 3091-3095.
- (24) Li, X.; Zhang, H.; Mai, Z.; Zhang, H.; Vankelecom, I. Ion exchange membranes for vanadium redox flow battery (VRB) applications. Energy Environ. Sci. 2011, 4 (4), 1147-1160.
- (25) Villarreal, M. S.; Kharisov, B.; Torres-Martinez, L.; Elizondo, V. Recovery of vanadium and molybdenum from spent petroleum catalyst of PEMEX. Ind. Eng. Chem. Res. 1999, 38 (12), 4624-4628.
- (26) Gattrell, M.; Park, J.; MacDougall, B.; Apte, J.; McCarthy, S.; Wu, C. Study of the mechanism of the vanadium 4+/5+ redox reaction in acidic solutions. J. Electrochem. Soc. 2004, 151 (1), A123-A130.
- (27) Wu, C.-H.; Liao, H.-Y.; Hsueh, K.-L.; Hung, J.-S. Study of the kinetics of vanadium redox reaction by rotating disk electrode. ECS Trans. 2011, 35 (32), 11-22.
- (28) Aureliano, M.; Crans, D. C. Decavanadate (V₁₀O₂₈⁶⁻) and oxovanadates: Oxometalates with many biological activities. J. Inorg. Biochem. 2009, 103 (4), 536-546.
- (29) Khan, M. I.; Chen, Q.; Goshorn, D.; Zubieta, J. Polyoxo alkoxide clusters of vanadium: structural characterization of the decavanadate core in the" fully reduced" vanadium (IV) species 3 C C H 2 C H 3 } 4] 4 $V_{10}O_{16}\{(OCH_2)$ Chem. 1993, 32 (5), 672-680.
- (30) Ramasarma, T., The emerging redox profile of vanadium. Proceedings-Indian National Science Academy Part B 2003, 69 (4), 649-
- (31) Patole, M.; Gullapalli, S.; Ramasarma, T. Vanadate-stimulated NADH oxidation requires polymeric vanadate, phosphate and superoxide. Free Radical Res. Commun. 1988, 4 (4), 201-207.
- (32) Crans, D. C.; Bunch, R. L.; Theisen, L. A. Interaction of trace levels of vanadium (IV) and vanadium (V) in biological systems. J. Am. Chem. Soc. 1989, 111 (19), 7597-7607.
- (33) Crans, D. C. Aqueous chemistry of labile oxovanadates: relevance to biological studies. Comments Inorg. Chem. 1994, 16 (1-2), 1 - 33.

- (34) Leinweber, P.; Meissner, R.; Eckhardt, K. U.; Seeger, J. Management effects on forms of phosphorus in soil and leaching losses. *Eur. J. Soil Sci.* 1999, 50 (3), 413–424.
- (35) Slack, A. V. Phosphoric Acid; Marcel Dekker, Inc.: New York, 1968; Vol. 1.
- (36) Zhang, Y.; Muhammed, M. The removal of phosphorus from iron ore by leaching with nitric acid. *Hydrometallurgy* **1989**, 21 (3), 255–275.
- (37) Liu, H.; Kuznetsov, A. M.; Masliy, A. N.; Ferguson, J. F.; Korshin, G. V. Formation of Pb (III) intermediates in the electrochemically controlled Pb (II)/PbO₂ system. *Environ. Sci. Technol.* **2012**, 46 (3), 1430–1438.
- (38) Kim, J.; Korshin, G. V.; Frenkel, A. I.; Velichenko, A. B. Electrochemical and XAFS Studies of Effects of Carbonate on the Oxidation of Arsenite. *Environ. Sci. Technol.* **2006**, *40* (1), 228–234.
- (39) Ma, J.; Yan, M.; Kuznetsov, A. M.; Masliy, A. N.; Ji, G.; Korshin, G. V. Rotating Ring-Disk Electrode and Quantum-Chemical Study of the Electrochemical Reduction of Monoiodoacetic Acid and Iodoform. *Environ. Sci. Technol.* **2015**, 49 (22), 13542–13549.
- (40) Jing, Y.; Chaplin, B. P. A Mechanistic Study of the Validity of Using Hydroxyl Radical Probes to Characterize Electrochemical Advanced Oxidation Processes. *Environ. Sci. Technol.* **2017**, *51* (4), 2355–2365.
- (41) Bard, A. J.; Faulkner, L. R. Electrochemical Methods: Fundamentals and Applications, 2nd ed.; Wiley: New York, 2000.
- (42) Babu, G. R.; Rao, P.; Ramakrishna, K.; Syamala, P.; Satyanarayana, A. Kinetics of oxidation of iron (II) by vanadium (V) under the conditions where VO₂⁺ and decavanadate coexist. *Int. J. Chem. Kinet.* **2000**, 32 (9), 535–541.
- (43) Sato, H.; Yui, M.; Yoshikawa, H. Ionic Diffusion Coefficients of Cs⁺, Pb²⁺, Sm³⁺, Ni²⁺, SeO₄²⁻ and TcO₄⁻ in Free Water Determined from Conductivity Measurements. *J. Nucl. Sci. Technol.* **1996**, 33 (12), 950–955.
- (44) Kalyani, P.; Ramasarma, T. A novel phenomenon of burst of oxygen uptake during decavanadate-dependent oxidation of NADH. *Mol. Cell. Biochem.* 1993, 121 (1), 21–29.
- (45) Gresser, M. J.; Tracey, A. S.; Parkinson, K. M. Vanadium (V) oxyanions: The interaction of vanadate with pyrophosphate, phosphate, and arsenate. *J. Am. Chem. Soc.* **1986**, 108 (20), 6229–6234
- (46) Williams, R. J. Metal ions in biological systems. *Biological Reviews* 1953, 28 (4), 381–412.
- (47) Rehder, D. Bioinorganic Vanadium Chemistry; John Wiley & Sons: New York, 2008; vol 30.
- (48) Zhang, B.; Feng, C.; Ni, J.; Zhang, J.; Huang, W. Simultaneous reduction of vanadium (V) and chromium (VI) with enhanced energy recovery based on microbial fuel cell technology. *J. Power Sources* **2012**, 204, 34–39.